Simulation of Membrane Heat Pump System Performance for Space Cooling

Ahmad A. Bukshaisha[a], Brian M. Fronk[a,*]

[a]*School of Mechanical, Industrial and Manufacturing Engineering*
Oregon State University
Corvallis, OR 97331 USA

Abstract

Membrane based heat pumps systems have attracted the attention of many research groups as a potentially more environmentally friendly alternative to vapor compression systems for space cooling. Several prototype systems have been developed, with reported claims of Energy Efficiency Ratios (EER) approaching 26. At present, no detailed analysis is publicly available which simulates the capability of these systems in different climate zones. In this work, a thermodynamic cycle model of a representative membrane heat pump system is developed and heat and mass transfer components are sized to provide 3 tons of cooling at nominal rating conditions. The performance of the 3 ton system is then simulated in various climate regions using representative cooling loads. The simulated membrane heat pump system had an EER of 16-20. Compared with the performance of a commercial vapor compression system, the membrane system performs better at higher dry-bulb temperature and shows energy saving potential in all climate regions examined. While

*Corresponding author
Email address: brian.fronk@oregonstate.edu (Brian M. Fronk)

the membrane system shows potential from a thermodynamic perspective, there are many practical challenges that must be addressed prior to commercialization including the design of an efficient vacuum pump, mitigating membrane fouling and reliability issues, and developing advanced controls to maintain desired sensible and latent heating capacities.
Keywords: Membrane heat pump, non-vapor compression, vacuum membrane dehumidification, HVAC, Simulation

---

1. Introduction

Heating, ventilation, and air conditioning (HVAC) consumes 48% of the total energy in buildings in the United States, with 12.3% dedicated to space cooling [1]. Vapor compression systems are used for space cooling in 90% of the buildings in the United States. A vapor compression heat pump relies on an evaporating and condensing refrigerant to transfer energy between thermal reservoirs. The refrigerant is evaporated at a low pressure (removing heat from a conditioned space), and compressed to a high pressure vapor where it is condensed, rejecting heat from the system. The fluid is then expanded back to a lower pressure and the cycle repeats. This basic cycle has been in use for over one hundred years, yielding very reliable, efficient equipment. However, the work of compression is high, and the working fluids are often not environmentally friendly. Common refrigerants such as R-134a and R-410A are in the process of being phased out due to their high global warming potential (GWP), where they have a GWP of 1430 and 2088, respectively [2]. Thus, there has been significant interest in the investigation of non-vapor compression technology for cooling. One of the promising technologies

identified by the United States Department of Energy (DOE) is the use of membrane based systems capable of transferring sensible and latent energy [3]. An example of a potential system configuration is shown in Figure 1, as reported in Goetzler et al. [4] and based on research conducted by DAIS Analytic.

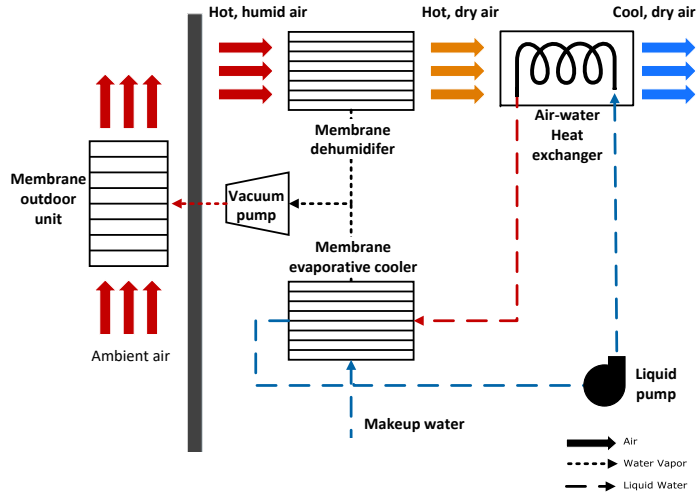

Figure 1: Schematic of membrane heat pump system with labeled state points

The system couples a membrane vacuum dehumidification system with a membrane based indirect evaporative cooler. A vacuum pump creates a low vapor pressure to remove moisture from the supply air and from the indirect evaporative cooler loop, as shown. Then the vacuum pump discharges the water vapor to a third membrane module which transfer moisture to the ambient air. Therefore, the vacuum pump needs to compress the water vapor to the ambient water vapor partial pressure and not the absolute, hence reducing the compression ratio from ˜100 to approximately 3-5. High

energy efficiency ratio (EER) of this and similar membrane based cycles have been reported [4], however, there are no detailed published performance data in the open literature. Thus, the objective of this work is to expand upon prior work [5] and develop a simulation model of the membrane heat pump concept shown in Figure 1 and then use it to predict seasonal performance in different climate regions within the United States. Energy performance ratings such as coefficient of performance (COP), and EER, as well as utility costs will be evaluated for different geographic locations. These results are then compared to conventional, high efficiency, vapor compression systems.

2. Prior Work

Membranes have been used in many different HVAC devices [6], including membrane based energy recovery ventilators, vacuum membrane dehumidification systems, and membrane based liquid desiccant dehumidifiers. Of these, vacuum membrane dehumidification systems are most relevant to the membrane heat pump system described in Section 1. In this type of system, a pressure gradient is created across two sides of a membrane using a compressor/vacuum pump. The vacuum pump lowers the partial pressure of water vapor in the permeate side, which causes moisture to transfer from the retentate (ambient air) side, drying the process air. An early use of the technology was be NASA for recovering moisture from air during space travel [7]. By integrating vacuum dehumidification system into HVAC equipment, sensible and latent cooling functions can be decoupled, which potentially enables novel control algorithms and system configurations to be developed that are more energy efficient. The key for membrane systems to be successful in

HVAC applications are the availability of materials with high permeability and high selectivity for water vapor. Membrane permeability is a measure of the resistance to transport of the desired species through a material for a given driving force, while selectivity is related to the ratio of the permeability of the membrane for the desired (water vapor) and undesired (air) species.

El-Dessouky et al. [8] was one of the first groups to explore integrating membrane dehumidification systems into an air conditioning setup. Their system consisted of a vacuum membrane dehumidifier, indirect evaporative cooler, and direct evaporative cooler arranged in series. Hot humid air enters the membrane module where it is dehumidified and then pre-cooled in the indirect evaporative cooler, before being brought to the final wet-bulb and dry-bulb temperature in the direct evaporative cooler. They concluded that the modeled system had the potential for an 86% reduction in energy consumption compared to a standard vapor compression system, assuming a membrane selectivity (water/nitrogen) of 400 and a permeate vacuum pressure of 10 kPa. They stated that energy savings could be increased with higher performing membranes.

Zhao et al. [9] built a test apparatus for evaluating membrane material performance during vacuum dehumidification. They considered an architecture of 9 bundles, each containing one inch hollow fiber membranes. One side of the membrane array was exposed to vacuum and the other to ambient air. They ran the system for 150 hours to evaluate humidity removal, durability, and energy savings, and found the potential for a reduction of 26.2% in energy consumption compared to a vapor compression system. Interestingly, the selectively of the membrane bundles in their experiments were very low,

around 2, and the permeate pressure pressure was approximately 78 kPa. In a detailed study on membrane properties, Bui et al. [10] showed that it was possible to remove sufficient moisture with low selectivity membranes, but at the expense of low membrane COP (i.e., the ratio of the latent energy removed divided by vacuum pump work).

A downside of both of the systems described above is that the driving force across the membrane is relatively low, primarily due to the relatively high permeate absolute pressure of between 10 and 78 kPa. Woods [6] suggests that the permeate water vapor pressure should be reduced to 1.25 kPa for sufficient driving force. However, when the water vapor is then discharged to ambient pressure, this would result in very large compression ratios, requiring the use of 2-stage pumps that would not be feasible for HVAC applications. Scovazzo and Scovazzo [11] addressed this issue through the use of a vacuum sweep humidification (VSD) system. Here, some of the retentate (dehumidified air) is used as a sweep gas on the permeate side to reduce the partial pressure of water vapor (˜1.25 kPa) while maintaining reasonable absolute pressure (˜20 kPa) to minimize compression ratio. This was accomplished by forcing some fraction of the retentate stream through a throttling valve into the permeate side which reduces the vapor partial pressure significantly while increasing the absolute pressure, thereby reducing the compression ratio from a typical value of 80-100 to 5-10. They measured the system's humidity removal capability and compared it to a commercially available 2-stage vapor compression system coupled with desiccant cycle for energy recovery. Although using some of the retentate as a sweep gas reduces the system's performance, Scovazzo and Scovazzo [11] showed that the system

is capable of matching the existing systems humidity removal and can reach a dehumidification efficiency of greater than 200%. However, the use of a sweep gas causes an increase in power required, resulting in a trade off between humidity removal and dehumidication efficiency. Therefore, the sweep rate must be optimized depending on the specific application.

Another solution to avoid high compression ratio, without affecting the system's performance, is to discharge the water vapor from the permeate side into another membrane module at some intermediate pressure instead of directly to ambient pressure, as described in Section 1. A system built on this concept has been developed by DAIS Analytic starting with an initial project funded by the United State Department of Energy ARPA-E program in 2009. With this approach, the water vapor pressure in the permeate side needs to be compressed to a pressure that is few pascals higher than the ambient vapor pressure, which in HVAC applications is typically around 3-5 kPa. Due to this compression ratio reduction, the initial concept was reported to have very high energy efficiency ratios compared to vapor compression systems [4]. However, the lack of data in different climate regions motivates the need for the present investigation.

3. Model Development

3.1. Approach

To simulate the performance of the membrane system, an initial thermodynamic state point model was developed in *Engineering Equation Solver* (EES) [12] for a 3 ton cooling capacity and other assumed parameters at a nominal rating condition. Using this model, the physical size of the heat

and mass exchangers and vacuum pump power at the nominal condition were determined. These values were then used as inputs into a more detailed physical model, which enabled the performance of the heat pump to be simulated under varying ambient conditions in different climate regions. The results of this model were compared to the seasonal performance of a representative vapor compression system using performance curves from a commercially available product.

3.2. Description of the Modeled System

The membrane heat pump concept investigated in this paper was shown previously in Figure 1, and was developed by DAIS Analytic, as reported in [4]. Starting at state point 1 in Figure 1, hot humid return air from the conditioned space enters the membrane dehumidifier. The vacuum pump creates the required differential pressure, which extracts the moisture from the air through the selective membrane, resulting in latent heat removal. Then, the hot, dry air passes through the chilled water coils, removing sensible heat and cooling the air down to the design supply dry-bulb temperature before entering the conditioned space (state point 3). The sensible cooling load is rejected through an evaporative cooling process at the membrane evaporative cooler, where water vapor from the circulating water loop is extracted by the vacuum pump (state 4 to 5) to maintain the circulating water temperature. The water vapor extracted from both the membrane dehumidifier and membrane evaporative cooler is rejected to the ambient through a third selective membrane humidification process by compressing the water vapor to a slightly higher pressure than the ambient partial vapor pressure. Finally, makeup water is added to the circulating coolant loop (state 13). The cool-

ing process in this membrane heat pump system does not use any working fluid other than water, eliminating the use of high global warming potential working fluids. Furthermore, enables the possibility of controlling the dry-bulb and wet-bulb temperature separately to maximize energy efficiency and thermal comfort.

3.3. State Point Simulation Model

The initial state point model was developed in EES to provide 3 tons of cooling at the ASHRAE residential rating conditions [13], with other assumed parameters shown in Table 1. In addition, it was assumed that the system operated at steady state and that pressure drop through each component was negligible. The goal from this model was to predict the required overall heat and mass transfer coefficients for each component, the vacuum pump power($\dot{W}_{vac,pump}$), and the required indoor air volumetric flow rate ($\dot{V}_1$) to provide 3 tons of cooling and a 12.78°C (55°F) supply air temperature (state 3).

Table 1: Design conditions set for the membrane heat pump systems

Parameter	**Value**	**Unit**
$\dot{Q}_{cooling}$	3	Tons
T_{db} (indoor return)	26.7	$^{\circ}C$
T_{wb} (indoor return)	19.4	$^{\circ}C$
T_{db} (outdoor ambient)	35.0	$^{\circ}C$
T_{wb} (outdoor ambient)	23.7	$^{\circ}C$
T_{supply} (state 3)	12.8	$^{\circ}C$
$\dot{V}_{11}$ (outdoor air flow)	1350	$ft^3\,\mathrm{min}^{-1}$
$\epsilon_{dehumidifier}$	0.7	-
$\eta_{vac,pump}$	0.75	-
$\eta_{liq,pump}$	0.90	-
$\dot{m}_w$	0.2	kgs^{-1}
T_w	15	$^{\circ}C$

State point 1 is the return air from the conditioned space. Pressure, temperature and relative humidity are known from the rating conditions. Thus, all thermodynamic properties including humidity ratio are fully defined. The humidity ratio at the outlet of the membrane humidifier is determined from the assumed effectiveness, as shown in Equation 1. The air pressure is assumed to remain constant.

$$\omega_2 = \omega_1 - \epsilon_{dehumidifier}\omega_1 \tag{1}$$

The water vapor from the membrane dehumidifier is removed to state point 7. Here, it is assumed that the water vapor temperature is equal to the humid air temperature at state 1, as the dehumidification process is approximately isothermal. The other property required at state point 7 is the pressure, which must to be less than the partial vapor pressure at state point 2. The initial simulation model defines the pressure at state 7 using the variable Z, as shown in Equation 2. A higher value of Z requires a high compression ratio, but yields a smaller heat and mass exchanger to achieve the same moisture removal. On the other hand, a smaller value of Z yields a larger heat and mass exchanger (smaller driving pressure differential), but decreases the required pressure ratio for the vacuum pump, increasing the COP. The assumed value of Z is 0.1, chosen from a trade off analysis between COP and size of the heat and mass exchanger [14]. This assumption is removed in the physical model, as the vacuum pump power and heat and mass exchanger size are fixed, as described below.

$$P_7 = P_{v2} - ZP_{v2} \tag{2}$$

The enthalpy at state 2 is calculated from an energy balance on the dehumidifier, as shown in Equation 3 below. The mass flow rate is calculated from Equation 4, where h_3 is evaluated using the design supply air temperature and ambient pressure, and ω_3 which is equal to ω_2. The specific enthalpies in Equations 3 and 4 are evaluated on a kJ per kg of dry air basis, by convention.

$$\dot{m}_a h_1 = \dot{m}_a[h_2 - (\omega_1 - \omega_2)h_7] \tag{3}$$

$$\dot{m}_a = \frac{\dot{Q}_{cooling}}{h_1 - h_3} \tag{4}$$

Similar mass and energy balances were performed for the air-water heat exchanger, membrane evaporative cooler, and outdoor membrane humidifier. To provide closure to the model, the closest approach temperature (CAT) and the closest approach pressure (CAP) were defined. The CAT is a design variable that constrains the minimum temperature difference between two streams in a heat exchanger, shown in Equation 5. The CAT was set to be 5°C after performing a parametric analysis on how it affects the system COP and heat exchanger size [14]. Similarly, the CAP is set to be 0.5 kPa to ensure that water vapor pressure at the vacuum pump exit is higher than the partial pressure at state point 12, shown in Equation 6, while maintaining a reasonable component size and system COP at the baseline condition.

$$T_6 = T_3 - CAT \tag{5}$$

$$P_{v10} = P_{v12} + CAP \tag{6}$$

After defining all state points in the EES model, the overall mass transfer coefficients (KA) of the membrane devices were evaluated using the vapor molar flow rate and the logarithmic partial pressure difference method as shown below:

$$\dot{n}_v = KA\Delta P_{v,LM} \tag{7}$$

$$\omega_i = 0.622\frac{P_{v,i}}{P_i - P_{v,i}} \tag{8}$$

Performing these calculations yielded the mass transfer coefficient, KA, for the membrane dehumidifier, membrane evaporative cooler and membrane humidifier. These KA values are a function of the physical membrane exchanger area, and the mass transfer resistances of the air/vapor streams and the membrane itself. Absent a more detailed design and simulation model, the KA value can be considered a surrogate for the size of the heat and mass exchanger. Similarly the UA of the heat exchanger was calculated using the logarithmic temperature difference and sensible load.

$$\dot{Q}_{HX3} = UA\Delta T_{LM} \tag{9}$$

$$\dot{Q}_{HX3} = \dot{m}_w(h_4 - h_6) \tag{10}$$

$$\dot{Q}_{HX3} = \dot{m}_a(h_2 - h_3) \tag{11}$$

The total work consumed by the system ($\dot{W}_{tot}$) was the sum of that done by the vacuum pump, liquid pump, indoor and outdoor fans, calculated using the equations below. Here, the pressure drop across the indoor (ΔP_{indoor}) and outdoor ($\Delta P_{outdoor}$) fan were both assumed to be 0.125 kPa (0.50 inches of water). The actual value would change depending on the design of the membrane devices. Lastly, the indoor air flow rate ($\dot{V}_1$) was obtained by dividing the total mass flow rate of the air at state point 1 by its density, as shown in Equation 16.

$$\dot{W}_{vac,pump} = \dot{m}_v(h_{10} - h_9) \tag{12}$$

$$\dot{W}_{liq,pump} = \dot{m}_w(h_6 - h_5) \tag{13}$$

$$\dot{W}_{indoor,fan} = \frac{\dot{V}_1 \Delta P_{indoor}}{\eta_{fan}} \tag{14}$$

$$\dot{W}_{outdoor,fan} = \frac{\dot{V}_{11}\Delta P_{outdoor}}{\eta_{fan}} \tag{15}$$

$$\dot{V}_1 = \frac{\dot{m}_1}{\rho_1} \tag{16}$$

All of the equations, mass and energy balances in this section were solved using an iterative process in EES to obtain results that satisfied the target design conditions for the membrane system. The results are summarized in Table 2, and were used as inputs to develop the physical model of the membrane heat pump system, discussed in the next section.

Table 2: Simulation model solution from EES

Parameter	**Value**	**Unit**
KA_1	$3.45 \cdot 10^{-4}$	$kmol\ s^{-1}kPa^{-1}$
KA_2	$3.95 \cdot 10^{-7}$	$kmol\ s^{-1}kPa^{-1}$
UA_{HX3}	0.506	kWK^{-1}
KA_4	$2.95 \cdot 10^{-4}$	$kmol\ s^{-1}kPa^{-1}$
$\dot{V}_1$ (indoor air flow)	565	$ft^3\,\mathrm{min}^{-1}$
$\dot{W}_{vac,pump}$	1.9	kW
$\dot{W}_{tot}$	2.2	kW

3.4. Fixed Physical Model

The individual component mass and heat transfer coefficients calculated in the previous section of this study were used as inputs in another model, the fixed physical model. This fixed physical model solves the thermodynamic

cycle using the same mass and energy balances as the previous section, except it uses the results highlighted in Table 2 as inputs instead of the assumed design values. The values for $\epsilon_{dehumidifer}$, CAT, CAP, T_{supply}, $\dot{Q}_{cooling}$, and Z were all substituted by the simulation model result values for KA_1, KA_2, UA_{HX3}, KA_4, $\dot{V}_1$ (indoor air flow rate), and $\dot{W}_{vac,pump}$ respectively. The COP and EER of the membrane heat pump system at the rating condition was then evaluated using Equations 17 and 18, which resulted in a COP and EER of 5.15 and 17.6, respectively.

$$COP = \frac{\dot{Q}_{cooling}}{\dot{W}_{tot}} \tag{17}$$

$$EER = \frac{\dot{Q}_{cooling}(Btuhr^{-1})}{\dot{W}_{tot}(W)} \tag{18}$$

3.5. Area Sizing Model

Before proceeding with the system simulation, it was desired to estimate the approximate size of the individual heat and mass transfer components to assess if they were physically realistic. Thus, a third model was developed to predict the approximate physical size of the heat and mass exchangers using estimates for the heat and mass transfer resistances within the components and membrane diffusivity and thickness. The membrane properties were similar to a recent study on membrane energy recovery ventilators conducted by Armatis and Fronk [15], with important parameters summarized in Table 3. These properties were selected as representative values of available membranes to provide an estimate of component size. For different membrane properties, the size of the components would change, but the thermodynamic analysis of interest in this paper remains valid.

The overall mass transfer coefficient, K, for each membrane component is defined in the model as the inverse of the supply and exhaust mass convective resistances and the membrane mass diffusivity, D_{mem}, added in series as shown.

$$K = \left(\frac{1}{k_s} + \frac{\delta_{mem}}{D_{mem}} + \frac{1}{k_e} \right)^{-1} \tag{19}$$

In Equation 19, the supply and exhaust mass transfer coefficients were evaluated using the Chilton-Colborn [16] analogy between heat and mass transfer, where the Nusselt number was assumed as 7.54 for fully developed laminar flow in parallel plates [17]. The analogy uses a correlation between the Sherwood number and Lewis number to calculate the mass transfer coefficient as shown below.

$$Sh = Nu \; Le^{-\frac{1}{3}} \tag{20}$$

$$k_{s,e} = \frac{Sh \; D_{air}}{D_h} \tag{21}$$

Here, the Lewis number can be approximated as 1.12 for HVAC applications [18], and D_{air} is the air mass diffusivity evaluated at the pressure, temperature and wet-bulb of the desired state point. This approach was used to evaluate the mass transfer coefficients for the membrane dehumidifier (indoor unit), membrane evaporative cooler, and the membrane humidifier (outdoor unit). The approximate required transport areas for the three components were then calculated by dividing the KA values, calculated from the simulation model, by the calculated overall mass transfer coefficients.

$$A_{HMX\,i} = \frac{KA_i}{K_i} \tag{22}$$

The assumed membrane properties and the resulting areas of the mass and heat exchangers are all summarized in the Table 3.

Table 3: Area sizing model solution with membrane properties

Variable	**Value**	**Unit**
A_{HMX1}	145	m^2
A_{HMX2}	0.16	m^2
A_{HMX4}	102	m^2
δ_{mem}	$50{\cdot}10^{-6}$	m
D_{mem}	$4.3{\cdot}10^{-7}$	$m^2 s^{-1}$
λ_{mem}	0.41	$W m^{-1} K^{-1}$
D_h	0.004	m

4. Model Analysis

4.1. Fixed Physical Model Analysis

In this section, parametric analysis were performed using the membrane physical model. Performance parameters such as COP and system cooling capacity at different indoor and outdoor conditions were evaluated, as well as the conditioned supply air temperature and humidity (state 3). The first parametric analysis performed was to evaluate the system performance at different outdoor relative humidity levels and outdoor dry-bulb temperatures. Figure 2a shows the system COP as a function of outdoor dry-bulb temperature and relative humidity, assuming a fixed indoor return air temperature

(state 1) from Table 1. For a given outdoor dry-bulb temperature, the system COP decreases as the relative humidity increases. At high relative humidity, the ambient partial vapor pressure increases, increasing the required pressure ratio across the vacuum pump and decreasing the cooling capacity. The COP decreases at fixed relative humidity as dry-bulb temperature increases for similar reasons. For this particular membrane system, the COP is always higher than 4.5 when the ambient dry-bulb temperature is less than 35°C (95°F). This shows that the system is capable of performing effectively in hot humid climates with acceptable COP.

Figure 2b shows the total, latent and sensible cooling capacities at two different outdoor dry-bulb temperatures and relative humidity from 0.1 to 0.9. Indoor return air conditions are fixed according to Table 1. Figure 2 shows that the membrane heat pump system latent cooling capacity decreases with increasing ambient relative humidity and dry-bulb temperature, while the sensible capacity is relatively unchanged. As the outdoor air humidity ratio increases, the required pressure ratio across the vacuum pump increases. This decreases the effectiveness of the membrane dehumidifier, decreasing latent capacity, while the indirect evaporative cooler performance is not as negatively affected, as the driving pressure difference is much larger.

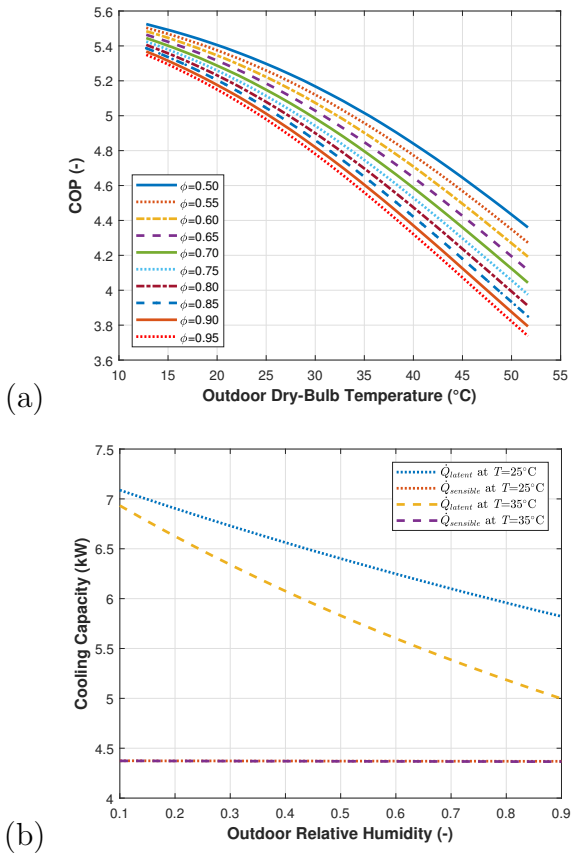

Figure 2: (a) Membrane heat pump system COP at different ambient conditions and (b) Membrane system total, latent and sensible cooling capacity at different ambient conditions

The last study performed with the physical model was to evaluate the supplied air temperature (state 3) and total cooling capacity when the indoor unit return dry-bulb and wet-bulb (state 1) are varied from the standard rating conditions. The results are shown in Figure 3a and 3b. Figure 3a shows that the supplied air dry-bulb temperature (state 3) increases as the return dry-bulb temperature increases (with fixed return wet-bulb at 19.4°C), while

the provided cooling capacity decreases, as would be expected. Interestingly, Figure 3b shows that the system provides more cooling with higher wet-bulb temperatures when the dry-bulb temperature is fixed at the rating condition, T=26.7°C. That is because a higher wet-bulb results in a larger partial pressure difference across the vacuum dehumidification device and the removal of more latent heat, resulting in a larger cooling capacity of the system. In the present study, there was no attempt to modulate the sensible or latent cooling capacity of the membrane system for different conditions. One can imagine that when more sensible cooling is required, the indirect evaporative cooling could be run independently of the membrane dehumidification device, and vice versa, to obtain optimal performance.

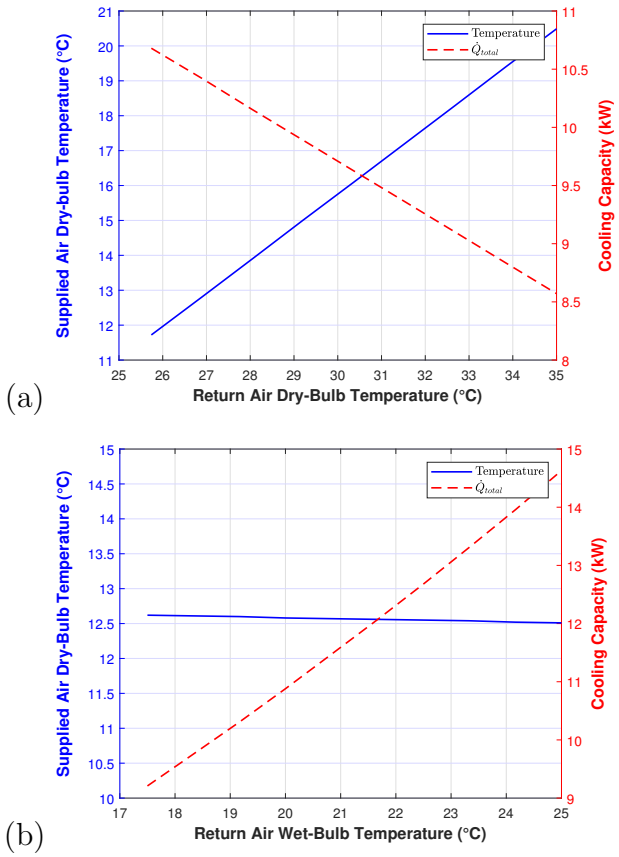

Figure 3: Membrane system supplied air-dry bulb temperature and total cooling capacity versus (a) indoor return air dry-bulb and (b) indoor return air wet-bulb

4.2. Membrane System Performance in Different Climates

To evaluate the membrane heat pump system performance in different climate regions in the US, a representative 2000 square foot building was specified in the building energy modeling software eQUEST [19]. Building parameters such as R-values of the roof and windows, window type, lighting, etc., were selected to result in a maximum required 3 tons of cooling for Phoenix. This same building was then used in ten different cities. In reality,

building parameters would be somewhat different in each city depending on the local climate. Still, using the same building to estimate the required cooling load provides an apples-to-apples comparison between the membrane and vapor compression system in each city, even if the actual required cooling load may be different with a different building construction.

The hourly cooling load for the building was predicted for 10 different cities in 6 climate zones within the United States. The 10 cities that were chosen for this study were: Atlanta, Chicago, Houston, Los Angeles, Madison, WI, Miami, Minneapolis, Phoenix, Portland, OR and Washington D.C. For each hour of the year and for each location, the COP, EER, sensible, latent and total cooling capacity of the membrane system were simulated with the physical model described above, using the local hourly ambient dry-bulb and wet-bulb as inputs, and assuming ASHRAE indoor rating conditions from Table 1. The total system run time and related electric consumption were calculated by dividing the hourly building load from eQUEST by the predicted total system cooling capacity from the membrane system simulation for that hour. The annual run time for each city is presented in Figure 4a. As expected, Miami, which has a hot and humid climate, had the maximum hours of operations at 2657 hr, whereas Madison, WI, which is colder, had the least at 992 hr. In addition to the run time required, the annual electric consumption for each city, as well as the approximate cost using the average electric rate for each city [20] is reported in Figure 4b.

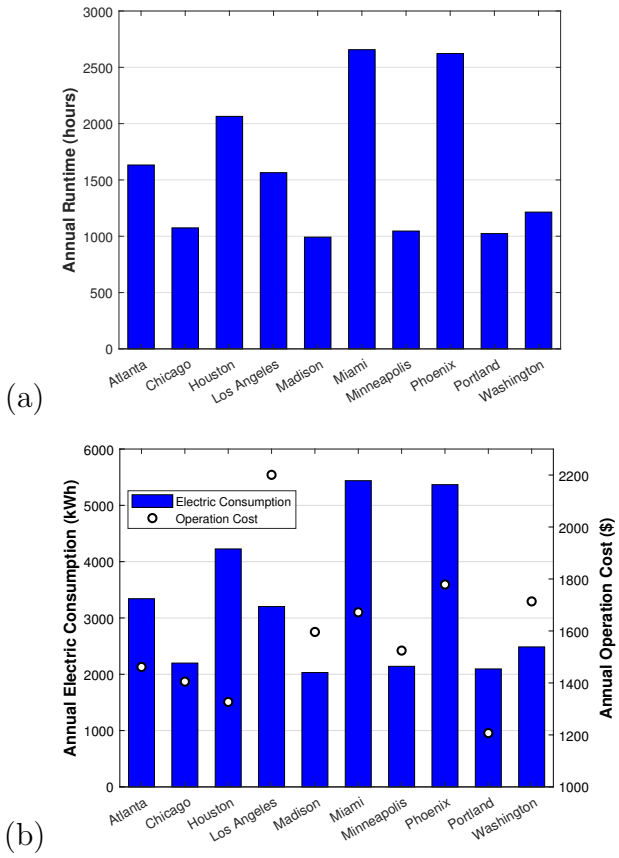

Figure 4: (a) Membrane system annual run time, (b) Membrane system annual electric consumption and costs

4.3. Comparison with Vapor Compression Systems

In this section, the membrane heat pump system is compared to conventional vapor compression systems. Performance parameters, such as the COP and the total cooling capacity, are compared to two commercially available vapor compression systems with seasonal energy efficiency ratio (SEER) values of 14 and 16, and each with a nominal cooling capacity of 3 tons. Using manufacturer performance data for representative systems [21, 22], the cool-

ing capacity, system power, and cooling COP could be evaluated at different combinations of outdoor dry-bulb, indoor wet-bulb, and indoor dry-bulb. These values were then be compared to the calculated values for the membrane system at the same conditions.

Figures 5a and 5b show how the membrane system COP compared with the vapor compression systems at different outdoor dry-bulb temperatures and two different indoor return air dry-bulb temperatures. For all cases, the outdoor wet-bulb temperature was fixed at 23.69°C and the indoor return wet-bulb at 21.67°C. The membrane heat pump is much less sensitive to outdoor dry-bulb variation temperature than the vapor compression systems. The COP of the membrane heat pump system was higher than 4.5 for the entire range of outdoor dry-bulb temperatures from 25°C to 50°C, whereas the vapor compression system COP decreased drastically from 5 to 2.3, or approximately a 50% drop for the same outdoor temperature range. These COP trends are due to the method of which heat is rejected to the ambient. For the vapor compression system, it is the outdoor dry-bulb which sets the compressor discharge temperature, whereas for the membrane system the vacuum pump discharge is governed by the outdoor wet-bulb. The membrane heat pump system, however, is more sensitive to the indoor supply air conditions compared to the vapor compression system. A change of 2.8°C (5°F) in the indoor unit supply dry-bulb temperature decreases the membrane system's COP by a maximum of 0.3, whereas it has a negligible effect on the vapor compression system COP.

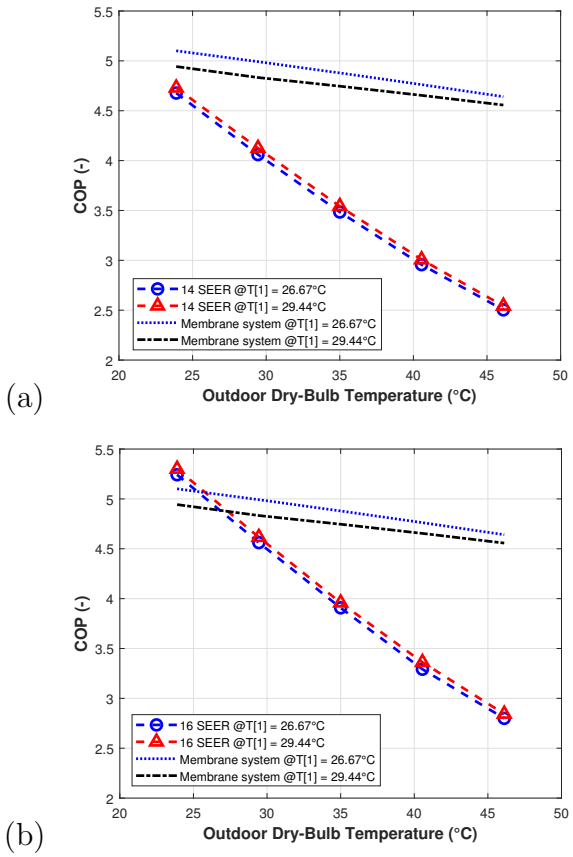

Figure 5: Membrane and vapor compression system COP versus outdoor dry-bulb temperature at outdoor wet-bulb of 23.69°C and indoor wet-bulb of 21.67°C for (a) 14 SEER vapor compression system and (b) 16 SEER vapor compression system

Figure 6 shows the total cooling capacity versus outdoor dry-bulb temperature for the membrane systems and the 14 and 16 SEER vapor compression systems. The outdoor wet-bulb temperature was constant at 23.69°C and the indoor return conditions were fixed at 26.67°C dry-bulb and 19.4°C wet-bulb. The total cooling capacity of the three systems follow a similar trend as the COP trends in Figure 5a and 5b. The membrane system's cooling capac-

ity does not drop significantly over the outdoor dry-bulb temperature range compared to the vapor compression systems. The membrane system generally provides less cooling compared to the vapor compression system at lower temperature, however, it is more stable overall over the large temperature range and provides more cooling at temperatures of 35°C and higher.

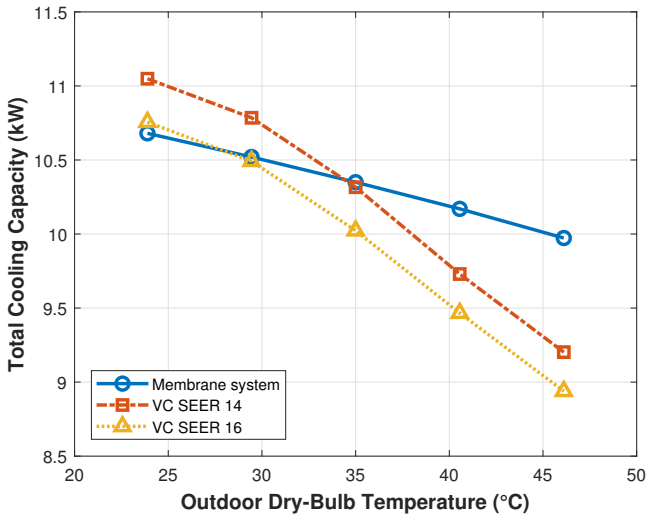

Figure 6: Membrane and vapor compression system total cooling capacity versus outdoor dry-bulb temperature at outdoor wet-bulb of 23.69°C and fixed indoor return air conditions of 26.67°C dry-bulb and 19.4°C wet-bulb

Figure 7 shows the sensitivity of the membrane system performance to indoor return air wet-bulb temperature. The COP of the membrane system and the 16 SEER VC system were evaluated at varied indoor wet-bulb temperatures and three different dry-bulb temperatures (from 23.9°C to 46.1°C). The outdoor conditions were fixed at a dry-bulb of 26.67°C and a wet-bulb of 23.69°C. The Figure shows that the COP of both systems decreases with increasing return dry-bulb temperature. However, as indoor return wet-bulb

temperature increases, the COP of the membrane system increases at a faster rate compared to the vapor compression system, which remains almost flat. This is due to the increased capability of the membrane heat pump system to remove more latent heat at higher indoor humidity levels at a fixed outdoor condition, via membrane dehumidification, which increases the total cooling capacity provided while consuming almost the same work. Whereas, vapor compression systems are not able to provide significant additional cooling by removing more latent heat due to the condensation dehumidifying method (i.e., the minimum humidity ratio is set by the supply air temperature).

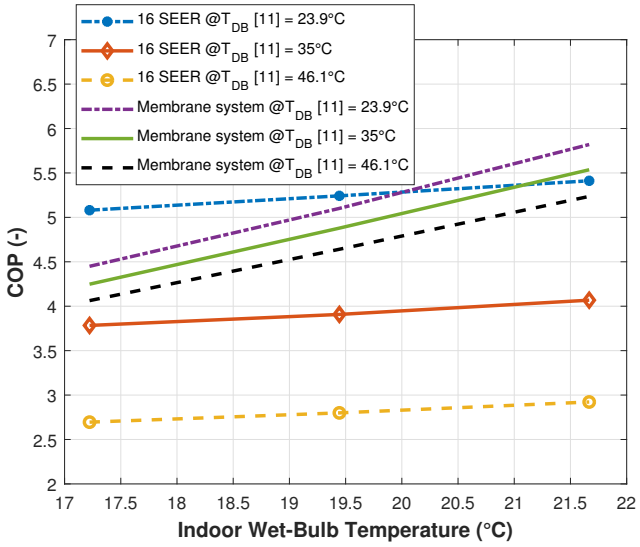

Figure 7: Membrane and vapor compression system COP versus indoor return air wet-bulb temperature at fixed outdoor conditions of 26.67°C dry-bulb and 23.69°C wet-bulb

4.4. Seasonal Performance Comparison of Membrane and Vapor Compression Systems

In this section, the seasonal performance of the membrane and vapor compression systems are compared. Using the commercial vapor compression

performance data as described above, functions for the total cooling capacity and compressor power were developed for the 16 SEER vapor compression system as a function of dry-bulb temperature. Then, using the weather file data from eQuest, the seasonal variation in cooling capacity and COP of the 16 SEER system could be predicted and the annual run time and energy consumption calculated for each of the 10 cities. The run time and electric consumption were evaluated using the same approach used for the membrane heat pump system, which is by dividing the required cooling load (calculated from eQuest) for the particular hour by the total cooling capacity of the system to get the run time, and then multiplying the run time by the work consumed to evaluate the electric consumption. The annual run time, electric consumption and energy savings were evaluated at three different operation scenarios. In the first scenario, it is assumed space cooling is only required if the ambient dry-bulb temperature is 68°F or higher, the second scenario is that cooling is required when the ambient dry-bulb is 72°F or higher, and in the final last scenario cooling is required when it is 77°F or higher. These scenarios values were chosen based on the suggested thermal comfort temperature range from ASHRAE which is between 67°F to 82°F [23]. The results for the annual run time, electric consumption and energy savings for both systems and all three scenarios are shown in Figures 8a, 8b and 9.

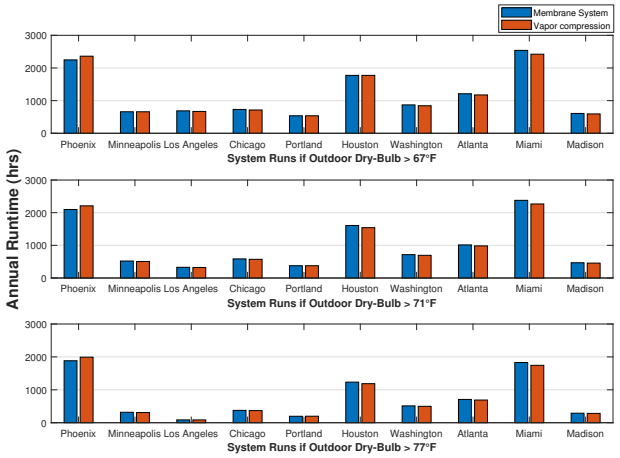

(a)

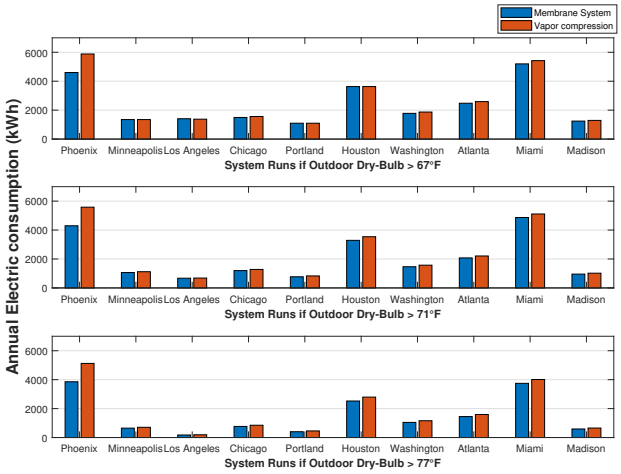

(b)

Figure 8: Comparison of (a) annual run time and (b) annual electric consumption for membrane system and 16 SEER vapor compression system for ten different cities

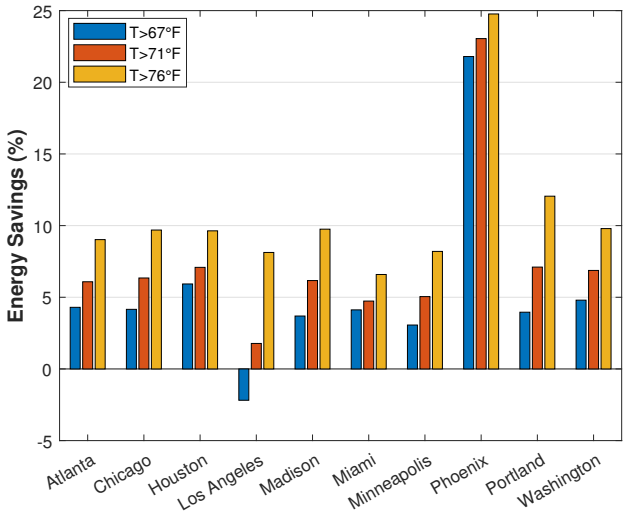

Figure 9: Annual energy savings of membrane system versus 16 SEER vapor compression system

Figure 8a shows that the required annual operation time does not vary significantly between the two systems for a given city. As expected, operation time is greater in hotter climates than in cooler. However, the results shown in Figure 8b reveal that while run time is similar there are differences in electrical energy consumption. Overall, the membrane heat pump system consumes less energy in all different climates for the 3 conditions, especially for scenarios where cooling was only required at outdoor dry-bulb higher than 77°F, which is when the COP of the membrane system is significantly higher than vapor compression system as shown in 5b. These differences in electric consumption are more easily evaluated in Figure 9, where the percent energy saved by the membrane system is shown for each city and for each cooling scenario.

The first scenario, where the systems operated at ambient of 67°F or

higher, showed the least savings for the membrane system. The membrane heat pump system had 3-5% energy savings for all cities except for Los Angeles and Phoenix where they had -2% and 22% energy savings, respectively. The reason for the negative savings in LA is because it had more hours of cooling at relatively low ambient temperatures compared to higher temperatures. As shown previously, at low temperatures the COP of the vapor compression system is higher, therefore for that case the vapor compression system performed better. On the other hand, Phoenix had more hours of high temperatures, where the membrane system outperformed the vapor compression system significantly.

The membrane system savings increase noticeably for the other two scenarios for all cities. This is because for these two scenarios the systems are not running at lower ambient temperatures, where the COP of the vapor compression system is higher than the membrane system. These results supports the conclusion made from Figure 5b where the membrane system were shown to have stable COP at high temperatures. Overall, the energy savings indicates how membrane systems can be a potential alternative to vapor compression systems, especially in hot climates like Phoenix. A possible reason why Phoenix resulted in the most significant energy savings is that the eQuest building model, used for all cities, was developed based on Phoenix climate weather, as described above. Buildings designed for the specific climate region in each city may require greater cooling loads, which would increase the energy savings percentage as the annual hours of run time increase.

The energy savings results in Figure 9 only accounted for the electric

consumption from the two systems. However, the membrane system requires makeup water, which as a utility cost and embodied energy cost. The annual water cost for the 10 cities investigated is shown in Figure 10, based on calculated consumed water and cost per gallon of water, excluding sewage costs. The annual water cost varied from one city to another, however the total water cost is very small compared to the total electric cost required for operating the membrane system shown in 4b. Los Angeles had the maximum water cost of $23, which is an insignificant addition to the electric cost which was around $2200. The utility water rate for each city was obtained from [24], where the rate is measured for a family of four 100 gallons is consumed per person per day.

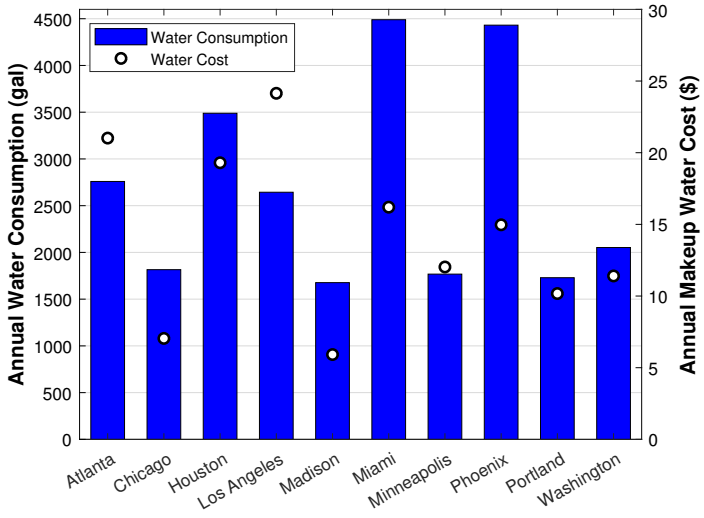

Figure 10: Annual makeup water cost for the 10 cities investigated

5. Conclusions and Practical Challenges

The membrane heat pump system investigated shows potential as an alternative to vapor compression systems as its performance is more stable over a wide range of outdoor dry-bulb temperatures while maintaining relatively high COP and EER over different climate zones. When comparing both systems in 10 different cities, the membrane heat pump system resulted in positive energy savings in all cities for scenarios when space cooling was required for outdoor ambient greater than 71°F.

However, inherent limitations of this study must be acknowledged. Changes in design assumptions (e.g., membrane component effectiveness, isentropic efficiency, etc.) would change the predicted efficiency and cost comparison with the vapor compression system. More detailed physical models of the membrane and sensible heat exchangers, as well as the vacuum pump would improve the accuracy of the comparison. Furthermore, only steady state operation of both systems were considered. It is unclear how quickly membrane systems would reach steady state, or what the efficiency during transients would be. Finally, an actual membrane based system would likely employ more sophisticated controls to decouple sensible and latent cooling functions, which could further change the comparison with vapor compression systems. Despite some of these limitations, this study shows qualitatively how a membrane based system would be expected to perform compared to a vapor compression system. In particular, the relative insensitivity of COP to outdoor dry-bulb and sensitivity to outdoor wet-bulb would have important implications from a design and sizing perspective.

Finally, several of the practical challenges in developing membrane sys-

tems should be addressed. A key issue is membrane fouling. Membranes have been used for water treatment and process water production, prior to being considered for integration into HVAC applications [25]. Here, the major membrane fouling mechanisms were pore blocking and cake formation. Similar fouling issues were encountered on a membrane based air-to-air energy exchanger that was assessed experimentally by Engarnevis et al. [26]. The membranes are generally affected by airborne particulates, such as dust, that is hard to filter out from the air stream. These particulates contribute to an increase in the total mass and heat resistance across the membranes. Depending on the particle size, if they are relatively large compared to the membrane pore size, they can accumulate in the membrane surface creating a layer that can decrease the vapor permeation rate. These can be effectively removed by a cleaning process or filtering. On the other hand, when the particulates are small, they could penetrate through the pores. This can result in partial or full pore blockage, resulting in significant reduction in vapor transport which affects the overall performance of the membrane device. For the membrane heat pump systems, fouling is expected to occur during dusty weather if sufficient filtration is not provided, or in very humid climates if condensate accumulates in the outdoor membrane module [27] which could wet the surface and decrease transport.

In addition to fouling, cross over of oxygen, nitrogen or other molecules other than water vapor would affect the partial pressure of water in the vacuum loop, and increase the required power to maintain effective transport. This suggests that highly selective, reliable membranes are important. Finally, membrane systems require makeup water to be supplied and require

the development of an efficient vacuum pump that can manage the pressure ratio and required volumetric flow rate. Despite these challenges, membrane systems have potential advantages that are worthy of continued investigation and development.

6. Acknowledgments

The support of the Qatar Research Leadership Program in supporting Mr. Ahmad A. Bukshaisha is gratefully acknowledged.

References

[1] EIA. Heating and cooling no longer majority of u.s. home energy use. Retrieved from `https://www.eia.gov/todayinenergy/detail.php?id=10271`, 2013.

[2] EPA. Refrigerants update. Retrieved from `https://www.epa.gov/sites/production/files/documents/RefrigerantUpdates.pdf`, 2011.

[3] W. Goetzler, R. Zogg, J. Young, and C. Johnson. Alternatives to HVAC Technology. *ASHRAE Journal*, 26:12–23, 2014.

[4] J. Young C. Johnson W. Goetzler, R. Zogg. Energy Savings Potential and RD & D Opportunities for Non- Vapor-Compression HVAC. *Energy Efficiency & Renewable energy*, (March):3673, 2014. doi: 10.2172/1220817.

[5] A. A. Bukshaisha and B. M. Fronk. Simulation of seasonal performance of a membrane heat pump system in different climate regions. *Proceedings of the 17th International Refrigeration and Air Conditioning Conference at Purdue*, 2018.

[6] J. Woods. Membrane processes for heating, ventilation, and air conditioning. *Renewable and Sustainable Energy Reviews*, 33:290–304, 2014. doi: 10.1016/j.rser.2014.01.092.

[7] R. Ray, D. D. Newbold, S. B. McCray, D. T. Friesen, and M. Kliss. A novel membrane device for the removal of water vapor and water droplets

from air. In *International Conference On Environmental Systems*. SAE International, July 1992. doi: https://doi.org/10.4271/921322.

[8] H. T. El-Dessouky, H. M. Ettouney, and W. Bouhamra. A Novel Air Conditioning System: Membrane Air Drying and Evaporative Cooling. *Chemical Engineering Research and Design*, 78(7):999–1009, 2000. doi: 10.1205/026387600528111.

[9] B. Zhao, N. Peng, C. Liang, W. F. Yong, and T-S. Chung. Hollow Fiber Membrane Dehumidification Device for Air Conditioning System. *Membranes*, 5(4):722–738, 2015. doi: 10.3390/membranes5040722.

[10] Thuan Duc Bui, Feng Chen, Aqdas Nida, Kian Jon Chua, and Kim Choon Ng. Experimental and modeling analysis of membrane-based air dehumidification. *Separation and Purification Technology*, 144: 114–122, 2015. ISSN 18733794. doi: 10.1016/j.seppur.2015.02.019.

[11] P. Scovazzo and A. J. Scovazzo. Isothermal dehumidification or gas drying using vacuum sweep dehumidification. *Applied Thermal Engineering*, 50(1):225–233, 2013. ISSN 13594311. doi: 10.1016/j.applthermaleng.2012.05.019.

[12] S. A. Klein. Engineering equation solver. Madison, WI: F-Chart Software, 2017.

[13] ASHRAE. 2017 ashrae handbook - fundamentals. Atlanta, GA: ASHRAE, 2017.

[14] A. A. Bukshaisha. *Investigation of Seasonal Performance of a Membrane*

Heat Pump System in Different Climate Regions. Ms thesis, Oregon State University, 2018.

[15] P. D. Armatis and B. M. Fronk. Evaluation of governing heat and mass transfer resistance in membrane-based energy recovery ventilators with internal support structures. *Science and Technology for the Built Environment*, 23:912–922, 2017. doi: 10.1080/23744731.2017.1325705.

[16] T. H. Chilton and A. P. Colburn. Mass transfer (absorption) coefficients prediction from data on heat transfer and fluid friction. *Industrial and Engineering Chemistry*, 26:1183–1187, 1934.

[17] F. P. Incropera, D. P. DeWitt, T. L. Bergman, and A. S. Lavine. Fundamentals of Heat and Mass Transfer, Incropera 6e. 325:672–682, 2007.

[18] L. Z. Zhang, C. H. Liang, and L. X. Pei. Heat and moisture transfer in application scale parallel-plates enthalpy exchangers with novel membrane materials. *Journal of Membrane Science*, 325:672–682, 2008. doi: 10.1016/j.memsci.2008.08.041.

[19] DOE. viewed January 2017. from `http://www.doe2.com/equest`, 2017.

[20] EIA. Us. energy information administration - state electricity profiles. Retrieved March 3, 2018, from URL `https://www.eia.gov/electricity/state/`, 2018.

[21] Goodman. Gsz14 heat pump. Retrieved March 1, 2018, from URL `https://www.goodmanmfg.com/products/heat-pumps/14-seer-gsz14`, 2018.

[22] Goodman. Gsz16 heat pump. Retrieved March 1, 2018, from URL https://www.goodmanmfg.com/products/heat-pumps/16-seer-gsz16, 2018.

[23] ASHRAE. What are the recommended indoor temperature and humidity levels for homes? 2016.

[24] Circle of Blue. The price of water - 2010-2018 water rates data from 30 major u.s. cities, 2018. URL https://www.circleofblue.org/waterpricing/.

[25] W. Guo, H-H Ngo, and J. Li. A mini-review on membrane fouling. *Bioresource Technology*, 122:27–34, 2012. doi: 10.1016/j.biortech.2012.04.089.

[26] A. Engarnevis, R. Huizing, S. Green, and S. Rogak. Particulate fouling assessment in membrane based air-to-air energy exchangers. *Energy and Buildings*, 150:477–487, 2017. doi: 10.1016/j.enbuild.2017.05.046.

[27] O. Labban, T. Chen, Lienhard J. H. Ghoniem, A. F., and L. K. Norford. Next-generation HVAC: Prospects for and limitations of desiccant and membrane-based dehumidification and cooling. *Applied Energy*, 200: 330–346, 2017. doi: 10.1016/j.apenergy.2017.05.051.

List of Figures

List of Tables

Nomenclature

Symbols

A	area	m^2
COP	coefficient of performance	–
EER	energy efficiency ratio	–
D_h	hydraulic diameter	m
D_{mem}	membrane diffusivity	$m^2 s^{-1}$
h	specific enthalpy	$kJ\ kg^{-1}$
h_t	heat transfer coefficient	$W\ m^{-2}\ K^{-1}$
K	overall mass transfer coefficient	$kmol\ m^{-2}\ s^{-1} kPa^{-1}$
k	convective mass transfer coefficient	$m\ s^{-1}$
Le	Lewis number	–
MW	molecular weight	$kg\ mol^{-1}$
$\dot{m}$	mass flow rate	kg s^{-1}
Nu	Nusselt number	–
$\dot{n}$	molar flowrate	$kmol\ s^{-1}$
P	pressure	kPa

$\dot{Q}$	heat duty	kW
R	universal gas constant	$m^3\ kPa\ kmol^{-1}K^{-1}$
Sh	Sherwood number	–
T	temperature	°C
U	overall transfer coefficient	$W\ m^{-2}\ K^{-1}$
$\dot{V}$	volumetric flowrate	$ft^3\ min^{-1}$
$\dot{W}$	power	kW

Greek Letters

ω	humidity ratio	–
ϵ	dehumidifier effectiveness	–
ϕ	relative humidity	–
δ	thickness	m
ρ	Density	kg m^{-3}
η	pump/fan efficiency	–
λ	thermal conductivity	$Wm^{-1}K^{-1}$

Subscripts

$1, 2...n$	state point number
a	air

e	exhaust
i	index notation
liq	liquid
LM	logarithmic mean
mem	membrane
s	supply
tot	total
v	vapor
vac	vacuum pump
w	water